catalysts

MDPI

Article

A CeO_2/ZrO_2-TiO_2 Catalyst for the Selective Catalytic Reduction of NO_x with NH_3

Wenpo Shan [1,2], Yang Geng [3], Yan Zhang [1,2], Zhihua Lian [1] and Hong He [1,2,4,*]

1 Center for Excellence in Regional Atmospheric Environment, Institute of Urban Environment, Chinese Academy of Sciences, Xiamen 361021, China; wpshan@iue.ac.cn (W.S.); yzhang3@iue.ac.cn (Y.Z.); zhlian@iue.ac.cn (Z.L.)

2 Ningbo Urban Environment Observation and Research Station-NUEORS, Institute of Urban Environment, Chinese Academy of Sciences, Ningbo 315800, China

3 School of Environmental and Biological Engineering, Nanjing University of Science and Technology, Nanjing 210094, China; yanggeng_njust@163.com

4 State Key Joint Laboratory of Environment Simulation and Pollution Control, Research Center for Eco-Environmental Sciences, Chinese Academy of Sciences, Beijing 100085, China

* Correspondence: honghe@rcees.ac.cn; Tel./Fax: +86-10-62849123

Received: 30 September 2018; Accepted: 27 November 2018; Published: 30 November 2018

Abstract: In this study, $CeZr_{0.5}Ti_aO_x$ (with a = 0, 1, 2, 5, 10) catalysts were prepared by a stepwise precipitation approach for the selective catalytic reduction of NO_x with NH_3. When Ti was added, all of the Ce-Zr-Ti oxide catalysts showed much better catalytic performances than the $CeZr_{0.5}O_x$. Particularly, the $CeZr_{0.5}Ti_2O_x$ catalyst showed excellent activity for broad temperature range under high space velocity condition. Through the control of pH value and precipitation time during preparation, the function of the $CeZr_{0.5}Ti_2O_x$ catalyst could be controlled and the structure with highly dispersed CeO_2 (with redox functions) on the surface of ZrO_2-TiO_2 (with acidic functions) could be obtained. Characterizations revealed that the superior catalytic performance of the catalyst is associated with its outstanding redox properties and adsorption/activation functions for the reactants.

Keywords: Ce-based catalyst; stepwise precipitation; selective catalytic reduction; diesel exhaust; nitrogen oxides abatement

1. Introduction

NO_x (mainly NO and NO_2) in the atmosphere plays critical roles in the formation of severe air pollution problems, such as haze, acid rain, and photochemical smog. In the last few decades, great efforts have been devoted to the development of NO_x emission control technologies [1–3]. Selective catalytic reduction of NO_x with NH_3 (NH_3-SCR) has been widely applied for the removal of NO_x generated from stationary sources for many years, and it has also been used for the control of NO_x emission from diesel vehicles [2,4].

Catalysts play an important role in the development of NH_3-SCR technology [5,6]. Vanadium-based catalyst (especially V_2O_5-WO_3/TiO_2), with excellent SO_2 resistance, is the most widely used NH_3-SCR catalyst for NO_x emission control from power plants, and it was also applied on diesel vehicles as the first generation of SCR catalyst [4]. However, this catalyst system still has some problems, including the toxicity of active V_2O_5, narrow temperature window, and low thermal stability [2].

There has been strong interest in developing a vanadium-free catalyst that can be used on diesel vehicles [5–11]. Ce is a key component in three-way catalysts for emission control in automobiles for gasoline. CeO_2 provides an oxygen storage function through redox cycling between Ce^{3+} and

Ce^{4+}. In recent years, Ce has also attracted great attention for applications as a support [12,13], promoter [14–18], or main active component [19–26] for NH_3-SCR catalysts.

Pure Ce oxide is not suitable for use as an NH_3-SCR catalyst [27,28]. When Zr oxide was introduced into Ce oxide, the thermal stability and the oxygen storage capacity of the oxide could be significantly improved. Therefore, Ce-Zr oxide was investigated for NH_3-SCR [12,13,29–34]. In the NH_3-SCR reaction, both redox functions and acidic functions of the catalyst are needed [4,35]. Therefore, a high dispersion of active sites and close coupling of redox with acid sites is the way to design a highly efficient NH_3-SCR catalyst.

In this study, starting from a preparation of Ce-Zr oxide by the co-preparation method, we developed a Ce-Zr-Ti oxide catalyst using a stepwise precipitation approach, under the theoretical guidance of the close combination of the Ce-Zr oxide with strong redox functions and Ti oxide with excellent acid properties [4,5]. This obtained catalyst showed superior catalytic performance for NH_3-SCR.

2. Results and Discussion

2.1. NH_3-SCR Activity

Figure 1A presents the NO_x conversion over the catalysts with different Ti contents under a relatively high gas hourly space velocity (GHSV) of 200,000 h^{-1}. The $CeZr_{0.5}O_x$ just exhibited over 50% NO_x conversion in a narrow temperature range of 350–425 °C. When Ti was introduced, all of the Ce-Zr-Ti oxide catalysts exhibited much better activities. With the increase in Ti content, the low temperature firstly increased and then decreased. As a result, the $CeZr_{0.5}Ti_2O_x$ catalyst presented the best activity in a low temperature range, together with a high NO_x conversion in a wide temperature range. On the other hand, the variation in high temperature activity with Ti content was contrary to that of low temperature activity, with the activity of $CeZr_{0.5}Ti_2O_x$ slightly lower than those of the other Ce-Zr-Ti oxide catalysts in a high temperature range. In addition, adding Ti to the catalyst also enhanced the N_2 selectivity, and the Ce-Zr-Ti oxide catalysts all presented higher N_2 selectivity than $CeZr_{0.5}O_x$ (Figure 1B).

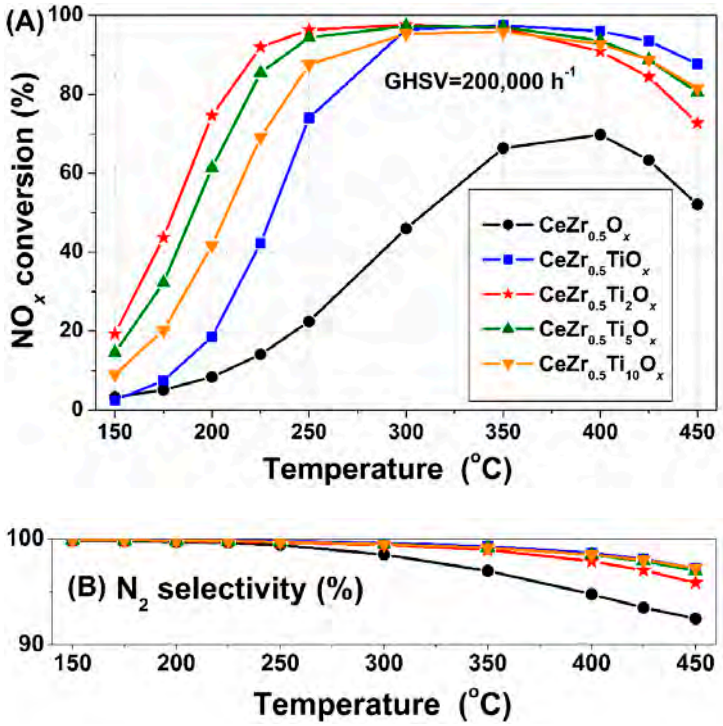

Figure 1. (**A**) NO_x conversions and (**B**) N_2 selectivity over the $CeZr_{0.5}O_x$ and Ce-Zr-Ti oxide catalysts. Reaction conditions: [NO] = [NH_3] = 500 ppm, [O_2] = 5 vol.%, N_2 balance, and GHSV = 200,000 h^{-1}.

The influences of H_2O and space velocity on the NO_x conversion over $CeZr_{0.5}Ti_2O_x$ were tested and the results are shown in Figure 2. The existence of 5% H_2O in the flow gas decreased the low temperature activity, but enhanced the high temperature activity. As a result, over 80% NO_x conversion could still be achieved from 250 to 450 °C. When the GHSV was decreased from 200,000 h^{-1} to 100,000 h^{-1}, the activity of the catalyst at low temperatures was obviously improved.

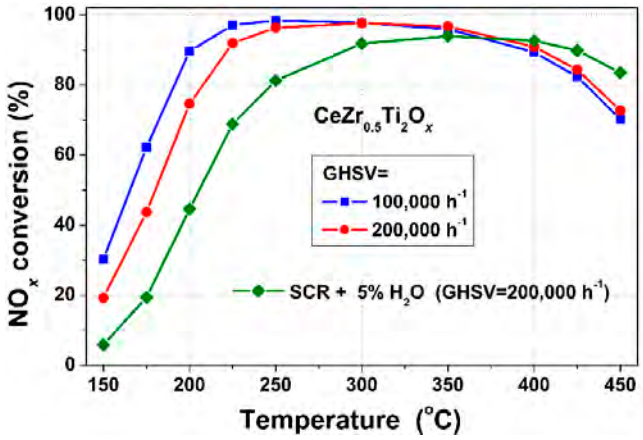

Figure 2. NO_x conversion over $CeZr_{0.5}Ti_2O_x$ catalyst under different reaction conditions. Reaction conditions: [NO] = [NH_3] = 500 ppm, [O_2] = 5 vol.%, [H_2O] = 5 vol.% (when used), N_2 balance, and GHSV = 100,000 or 200,000 h^{-1}.

2.2. Separated NO/NH_3 Oxidation

To analyze the effects of Ti on the catalyst, separated NO oxidation and NH_3 oxidation tests were carried out for the $CeZr_{0.5}O_x$ and $CeZr_{0.5}Ti_2O_x$ (Figure 3). The NO_2 production during NO oxidation over the $CeZr_{0.5}Ti_2O_x$ was clearly higher than that over $CeZr_{0.5}O_x$ at a low temperature. Since the presentation of NO_2 in the reaction gas could promote the SCR reaction at a low temperature by accelerating the fast SCR process (2 NH_3 + NO + NO_2 → 2N_2 + 3H_2O), the enhanced low-temperature activity by the introduction of Ti should be associated with the promoted oxidation of NO to NO_2 over $CeZr_{0.5}Ti_2O_x$ [10,35]. In addition, the introduction of Ti also promoted NH_3 oxidation over the catalyst at a high temperature. The NH_3-SCR reaction route at a high temperature mainly follows the Eley-Rideal mechanism, and the activation of NH_3 to form NH_2 species by oxidation plays the key role for the reaction with NO to form N_2 and H_2O, owing to NH_2 + NO(g) → N_2 + H_2O. Therefore, promoted NH_3 oxidation would be beneficial for the improvement of high temperature activity.

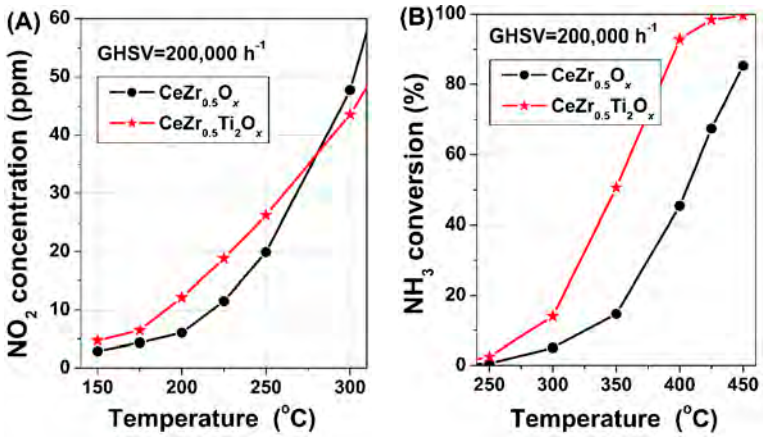

Figure 3. (**A**) NO_2 productions during separate NO oxidation reaction and (**B**) NH_3 conversions during separate NH_3 oxidation reaction over the $CeZr_{0.5}O_x$ and $CeZr_{0.5}Ti_2O_x$ catalysts. Reaction conditions: (A) [NO] _ENREF_30= 500 ppm, (B) [NH_3] = 500 ppm, [O_2] = 5 vol.%, N_2 balance and GHSV = 200,000 h^{-1}.

2.3. XRD

The X-ray diffraction (XRD) results of the $CeZr_{0.5}O_x$ and Ce-Z-Ti oxide catalysts are presented in Figure 4. Both CeO_2 and ZrO_2 were detected in $CeZr_{0.5}O_x$. With the increase of Ti, the peaks for CeO_2 and ZrO_2 became more and more weak, and only anatase TiO_2 was observed for $CeZr_{0.5}Ti_{10}O_x$. Only weak peaks for CeO_2 with cubic fluorite structures (PDF# 43-1002) were observed in the $CeZr_{0.5}Ti_2O_x$, indicating that the introduction of Ti had induced the structural change of the $CeZr_{0.5}O_x$, and the crystallizations of Ce, Zr and Ti oxides in $CeZr_{0.5}Ti_2O_x$ were significantly inhibited. As a result, the $CeZr_{0.5}Ti_2O_x$ (165.1 m^2/g) showed a higher Brunauer–Emmett–Teller (BET) surface area than $CeZr_{0.5}O_x$ (113.5 m^2/g).

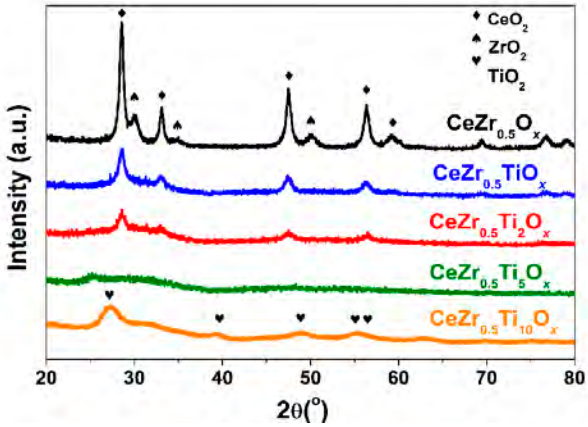

Figure 4. XRD patterns of the $CeZr_{0.5}O_x$ and Ce-Z-Ti oxide catalysts.

2.4. H_2-TPR

The H_2 temperature-programmed reduction (H_2-TPR) profiles of $CeZr_{0.5}O_x$ and $CeZr_{0.5}Ti_2O_x$ are presented in Figure 5. The $CeZr_{0.5}O_x$ exhibited two peaks at 496 and 755 °C due to the surface and bulk reductions of CeO_2 (as detected by XRD), respectively [31,36–38]. During the test, coordinatively unsaturated surface oxygen anions are easily reduced by H_2 in the low temperature region, while the bulk oxygen species are reduced only after the transportation to the surface [39]. With the addition of Ti, a sharp H_2 consumption peak appeared at 567 °C, which indicates that another type of Ce species might be formed. Considering the XRD results, this sharp peak might be associated with the reduction of the highly dispersed Ce species from Ce^{4+} to Ce^{3+} [22,34]. In addition, the H_2 consumption of $CeZr_{0.5}Ti_2O_x$ was much higher than that of $CeZr_{0.5}O_x$ at a low temperature. The H_2-TPR results clearly indicated the enhancement of redox functions for $CeZr_{0.5}Ti_2O_x$.

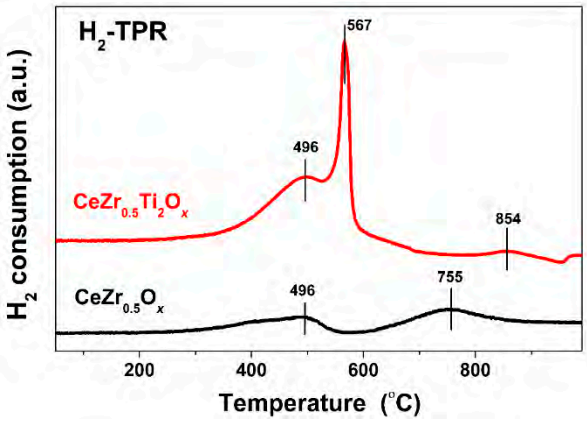

Figure 5. H_2-TPR profiles of the $CeZr_{0.5}O_x$ and $CeZr_{0.5}Ti_2O_x$ catalysts.

Previous studies have indicated that the redox properties of NH_3-SCR catalyst play a dominant role in the low temperature activity [35,40,41]. Therefore, the enhanced redox function of $CeZr_{0.5}Ti_2O_x$ would beneficial for low temperature activity.

2.5. NO_x/NH_3-TPD

To investigate the NO_x and NH_3 adsorption/desorption properties of $CeZr_{0.5}O_x$ and $CeZr_{0.5}Ti_2O_x$, NO_x temperature-programmed desorption (NO_x-TPD) and NH_3 temperature-programmed desorption (NH_3-TPD) were performed for the catalysts (Figure 6).

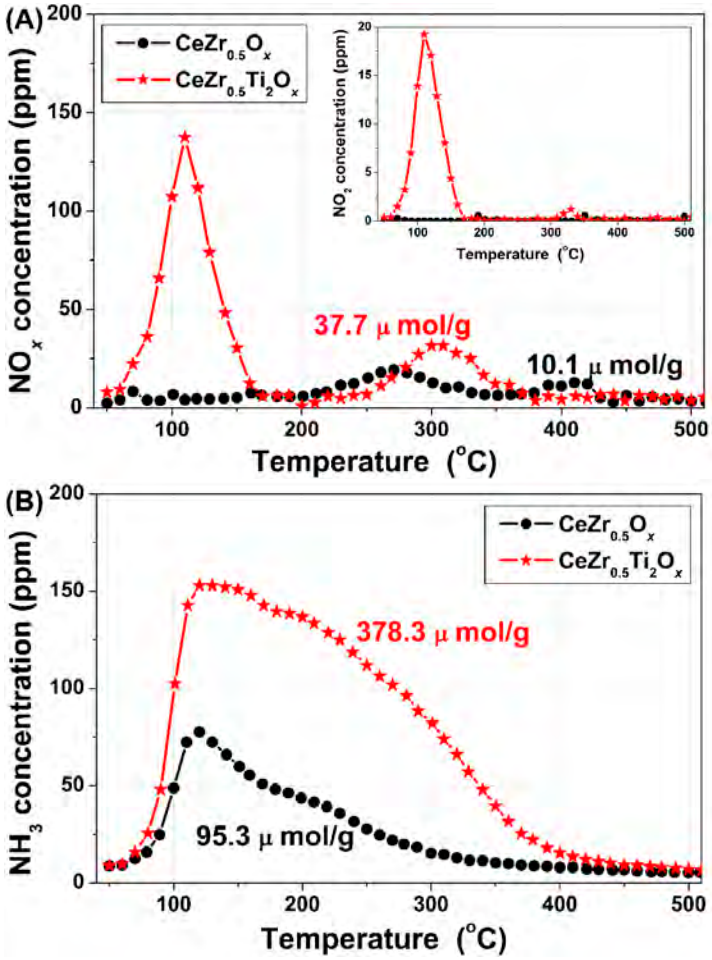

Figure 6. (**A**) NO_x-TPD and (**B**) NH_3-TPD profiles of the $CeZr_{0.5}O_x$ and $CeZr_{0.5}Ti_2O_x$ catalysts.

The NO_x-TPD profiles are presented in Figure 6A. The first NO_x peak of $CeZr_{0.5}Ti_2O_x$ was at ca. 110 °C, mainly due to the desorption of physisorbed NO_x, while the other NO_x peak was at ca. 300 °C and was associated with the decomposition of chemsorbed NO_x species [42,43]. On the other hand, two weak peaks were observed for $CeZr_{0.5}O_x$ at ca. 270 °C and ca. 410 °C, respectively, which were due to the decomposition of different types of chemsorbed NO_x species. With the addition of Ti, the adsorbed NO_x on $CeZr_{0.5}Ti_2O_x$ was obviously more than that of $CeZr_{0.5}O_x$. Particularly, the desorbed NO_2 of $CeZr_{0.5}Ti_2O_x$ was much higher, owing to the enhanced low-temperature activity for NO oxidation (as shown by the separated NO oxidation results), which could facilitate the conversion of NO_x in NH_3-SCR.

Surface acidity plays a dominate role in the high-temperature SCR activity due to its effects on the adsorption and activation of NH_3 [35,41]. Previous studies have revealed that Ti species of NH_3-SCR catalysts mainly act as acid sites in the reaction for NH_3 adsorption [4]. Therefore, the adsorbed NH_3

of $CeZr_{0.5}Ti_2O_x$ was much more than that of $CeZr_{0.5}O_x$, which might be an important reason for the better NH_3-SCR activity of $CeZr_{0.5}Ti_2O_x$ at high temperatures.

2.6. XPS

The X-ray photoelectron spectroscopy (XPS) results for Ce 3d of the $CeZr_{0.5}O_x$ and $CeZr_{0.5}Ti_2O_x$ are shown in Figure 7. The sub-bands labeled with u′/v′ and u^0/v^0 represent the $3d^{10}4f^1$ initial electronic state corresponding to Ce^{3+} and the $3d^94f^2$ state of Ce^{3+}, respectively [44]. The sub-bands labeled with u‴ and v‴ represent the $3d^{10}4f^0$ state of Ce^{4+}, and the sub-bands labeled with u, u″, v and v″ represent the $3d^94f^1$ state corresponding to Ce^{4+} [44]. The presence of Ce^{3+} would induce a charge imbalance, which could lead to unsaturated chemical bonds and oxygen vacancies. The calculated Ce^{3+} ratio of $CeZr_{0.5}Ti_2O_x$ (36.0%) was higher than that of $CeZr_{0.5}O_x$ (33.8%), indicating that more surface oxygen vacancies presented in $CeZr_{0.5}Ti_2O_x$. In addition, the Ce^{3+} ratio of the catalyst could influence the redox ability and reactant adsorption and activation functions, and thereby contribute to NH_3-SCR performance.

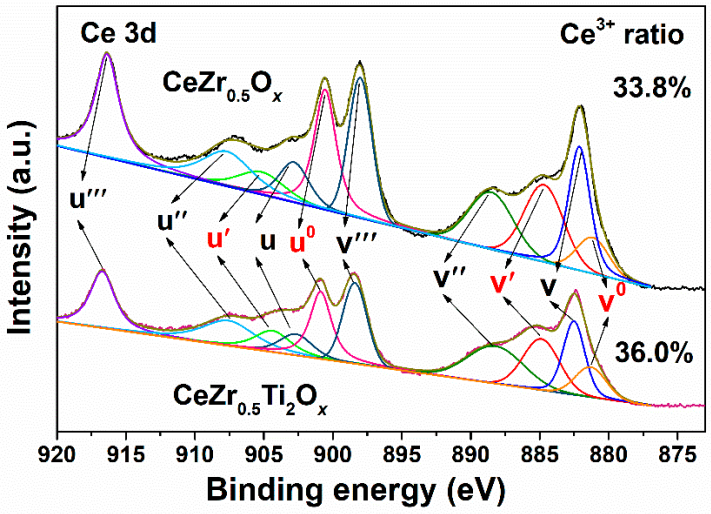

Figure 7. XPS results of Ce 3d of the $CeZr_{0.5}O_x$ and $CeZr_{0.5}Ti_2O_x$ catalysts.

The surface oxygen vacancies of the catalysts might generate weakly-adsorbed oxygen species or additional chemisorbed oxygen on the surface of the catalyst [27,45]. The XPS results of O 1s of the $CeZr_{0.5}O_x$ and $CeZr_{0.5}Ti_2O_x$ are shown in Figure 8. The O 1s peak was fit into two sub-bands. The sub-bands at 531.2–531.5 eV and 529.1–529.6 eV were assigned to the surface adsorbed oxygen (O_α), such as the O_2^{2-} and O^- belonging to defect-oxide or a hydroxyl-like group, and the lattice oxygen O^{2-} (O_β), respectively [46]. The O_α ratios of the catalysts were calculated by $O_\alpha/(O_\alpha + O_\beta)$, and the $CeZr_{0.5}Ti_2O_x$ showed higher O_α ratio than $CeZr_{0.5}O_x$. The results confirmed that the addition of Ti indeed induced more surface-adsorbed oxygen, which would facilitate NO oxidation to NO_2 (as shown by the separated NO oxidation and NO_x-TPD results), and thus facilitates the conversion of NO by fast SCR effects.

2.7. Formation Process Analysis of the $CeZr_{0.5}Ti_2O_x$ Catalyst

Figure 9 shows the pH variations of the mixed solutions for the preparation of the $CeZr_{0.5}O_x$ and $CeZr_{0.5}Ti_2O_x$ catalysts. During the preparation of $CeZr_{0.5}O_x$, the initial pH value of the solution was 1.6. With the hydrolysis of urea, the pH increased gradually to be 7.6 after heating for 12 h. Due to the increase in pH, suspended particles began to appear in the solution in the second hour. The particles with the precipitation time of 2 h, 4 h, 6 h, and 12 h were collected and then calcined to be catalyst samples. The activity tests of these samples showed similar NO_x conversions with each other.

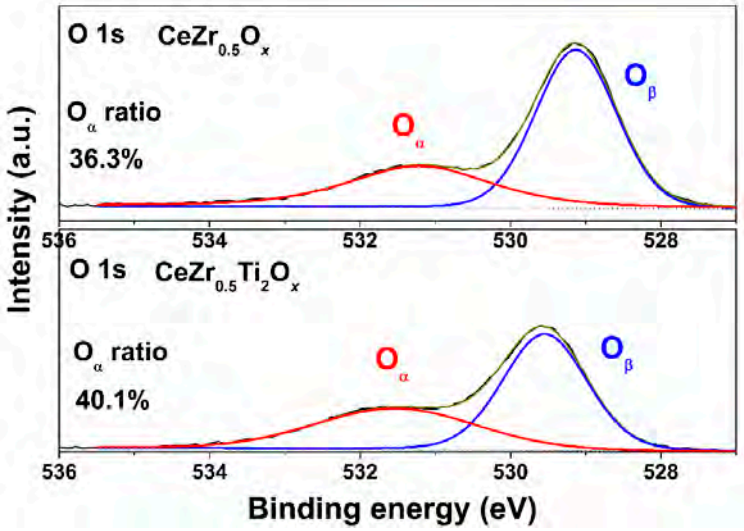

Figure 8. XPS results of O 1s of the $CeZr_{0.5}O_x$ and $CeZr_{0.5}Ti_2O_x$ catalysts.

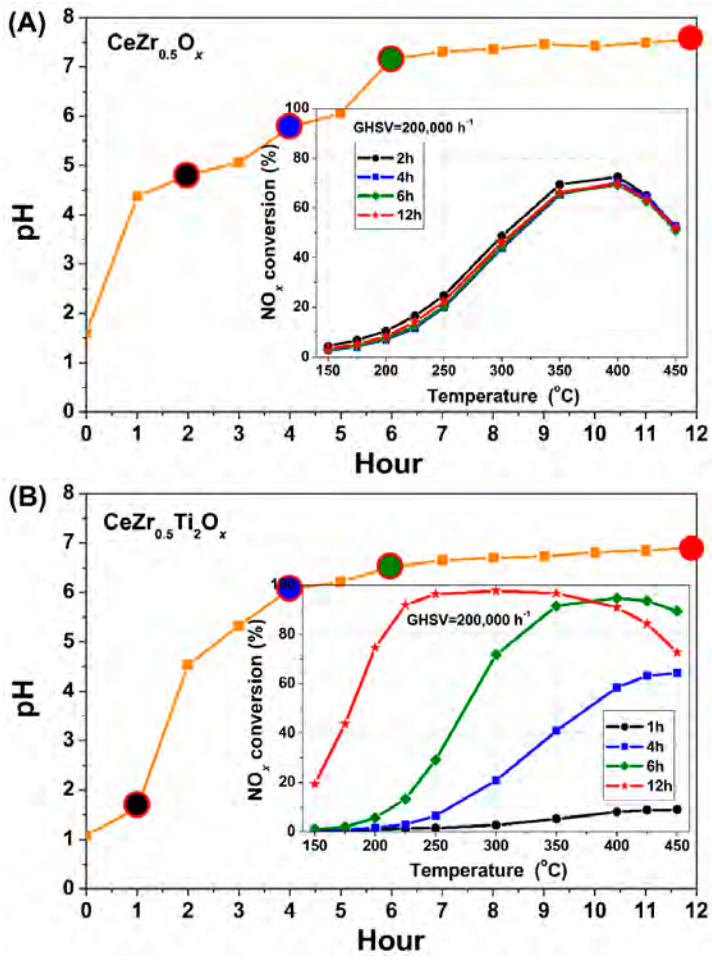

Figure 9. The pH variation of the mixed solution during the preparation of the (**A**) $CeZr_{0.5}O_x$ and (**B**) $CeZr_{0.5}Ti_2O_x$ catalysts, and the NO_x conversions of the obtained samples at different precipitation time.

Due to the acidity induced by the added $Ti(SO_4)_2$, the initial pH value of the mixed solution during the preparation of $CeZr_{0.5}Ti_2O_x$ dropped to be 1.1. With the hydrolysis of urea, the pH increased gradually after heating, and some white particles generated in the first hour and suspended in the

solution. With the increase of time, the particles gradually turned yellow. The pH reached ca. 7.0 after 12 h of reaction. The particles with the precipitation times of 1 h, 4 h, 6 h, and 12 h were collected and then calcined to be catalyst samples. Interestingly, the activity test showed a remarkable enhancement of NO_x conversions for the four samples with the increase in precipitation time.

The surface metal atomic concentrations of the $CeZr_{0.5}Ti_2O_x$ samples with different precipitation times were analyzed using XPS, and the variations in Ce, Zr, and Ti concentrations with precipitation time are shown in Figure 10. For the 1-h precipitation sample, only Ti and Zr, without Ce, were detected. With the increase in precipitation time, surface Ce concentration increased gradually in the samples. At the same time, Ti and Zr concentrations gradually decreased with the increase in precipitation time. A TEM-EDS mapping image showed that Ce was highly dispersed in the $CeZr_{0.5}Ti_2O_x$ catalyst (Figure 11).

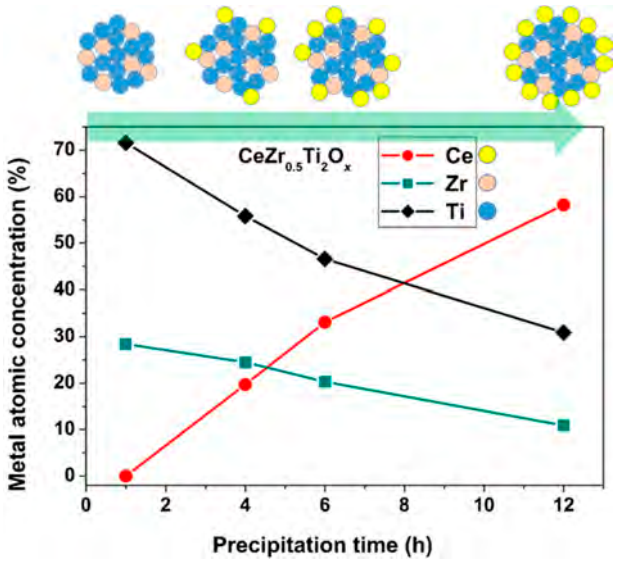

Figure 10. Surface metal atomic concentrations of the $CeZr_{0.5}Ti_2O_x$ samples with different precipitation times.

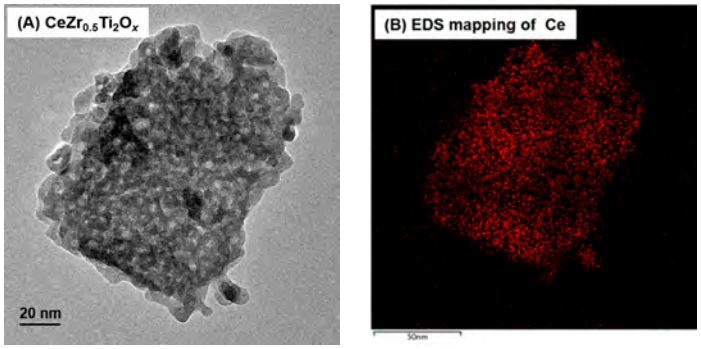

Figure 11. TEM image (A) and the corresponding EDS mapping (B) for the Ce of the $CeZr_{0.5}Ti_2O_x$ catalyst.

Considering the variations in the solution pH value when preparing the $CeZr_{0.5}Ti_2O_x$, the formation process of the catalyst can be proposed as follows: The Ti and Zr species were first co-precipitated with the increase in solution pH. Then, the Ce species uniformly precipitated onto the precipitated Zr-Ti species with the further increase in pH. Finally, a $CeZr_{0.5}Ti_2O_x$ catalyst with a higher surface Ce concentration than Ti and Zr was obtained. Through control of the hydrolysis of urea, the variations in the solution pH can be controlled, and then we can control the precipitation process of

the catalyst, which is very important for the formation of highly-dispersed CeO_2 on ZrO_2-TiO_2. Thus, the obtained catalyst can present excellent NH_3-SCR performance.

3. Experimental Section

3.1. Catalyst Preparation and Activity Test

The $CeZr_{0.5}Ti_aO_x$ (a = Ti/Ce molar ratio = 0, 1, 2, 5, 10), with a Zr/Ce molar ratio fixed to be 0.5, was prepared using a precipitation method. Desired precursors of $Ce(NO_3)_3{\cdot}6H_2O$ (>99%, Sinopharm Chemical Reagent Co., Ltd., Shanghai, China), $Zr(NO_3)_4{\cdot}5H_2O$ (>99%, Sinopharm Chemical Reagent Co., Ltd., Shanghai, China) and $Ti(SO_4)_2$ (>98%, Sinopharm Chemical Reagent Co., Ltd., Shanghai, China) were dissolved together in distilled water, and urea (>99%, Sinopharm Chemical Reagent Co., Ltd., Shanghai, China) was added to the mixed solution as a slowly-releasing precipitator. Then, the solution was heated to 90 °C to facilitate the release of NH_3 and thereby raise the pH value gradually. The temperature of the mixed solution was held at 90 °C for 12 h under vigorous stirring (some samples with shorter precipitation times were also prepared). After that, the precipitated powders were collected via filtration, washed using distilled water, and dried for 12 h at 100 °C. Finally, the catalyst was obtained after calcination at 500 °C for 5 h.

The SCR activity of the catalysts (40–60 mesh) were tested in a fixed-bed quartz flow reactor. The reaction conditions were controlled as follows: 500 ppm NO, 500 ppm NH_3, 5 vol.% O_2, N_2 balance, and 400 mL/min total flow rate. Different gas hourly space velocities (GHSVs) were obtained by changing the volume of catalysts, i.e., 0.24 mL catalyst for a GHSV = 100,000 h^{-1} and 0.12 mL catalyst for a GHSV = 200,000 h^{-1}. The concentrations of effluent N-containing gases (NO, NH_3, NO_2 and N_2O) were continuously measured by an online FTIR gas analyzer (Nicolet Antaris IGS analyzer, Thermo-Fisher Scientific, Waltham, MA, USA). NO_x conversion and N_2 selectivity were calculated using the following equations, respectively:

$$NO_x \text{ conversion} = (1 - \frac{[NO]_{out} + [NO_2]_{out}}{[NO]_{in} + [NO_2]_{in}}) \times 100\%$$

$$N_2 \text{ selectivity} = (1 - \frac{2[N_2O]_{out}}{[NO_x]_{in} + [NH_3]_{in} - [NO_x]_{out} - [NH_3]_{out}}) \times 100\%$$

3.2. Characterizations

X-ray diffraction (XRD) measurements were carried out on a computerized AXS D8 diffractometer (Bruker, GER), with Cu Kα (λ = 0.15406 nm) radiation, from 20 to 80° at 8°/min.

Surface areas were tested using an ASAP 2020 (Micromeritics, Norcross, GA, USA) at −196 °C by N_2 adsorption/desorption and calculated using a BET equation in the 0.05–0.35 partial pressure range.

The X-ray photoelectron spectroscopy (XPS) results of Ce 3d and O 1s were measured on an ESCALAB 250Xi Scanning X-ray Microprobe (Thermo-Fisher Scientific, Waltham, MA, USA) using Al Ka radiation (1486.7 eV) and a C 1 s peak, with BE = 284.8 eV as the calibration standard.

The transmission electron microscopy (TEM) image and energy-dispersive X-ray spectroscopy (EDS) mapping of Ce were obtained using a JEM-2100F equipment (JEOL, Tokyo, Japan), combined with a specimen tilting beryllium holder for energy dispersive spectroscopy. The accelerating voltage was 200 kV.

The H_2 temperature-programmed reduction (H_2-TPR) was tested using an AutoChem_II_2920 chemisorption analyzer (Micromeritics, Norcross, GA, USA), and the temperature-programmed desorption of NH_3 and NO_x (NO_x-TPD and NH_3-TPD) were tested using the same reaction system as the activity tests. Experiment details can be found in Reference [42].

4. Conclusions

A series of Ce-Zr-Ti oxide catalysts were prepared using a stepwise precipitation approach for NH_3-SCR. $CeZr_{0.5}O_x$ without Ti just showed a relatively low NO_x conversion. When Ti was introduced, Ce-Zr-Ti catalysts showed much better activities and N_2 selectivity. A $CeZr_{0.5}Ti_2O_x$ catalyst, which contains moderate Ti amounts, showed the best performance, which is associated with its optimal ratios for the redox (CeO_x) and acidic (TiO_2) components.

$CeZr_{0.5}O_x$ and $CeZr_{0.5}Ti_2O_x$ catalysts were characterized using various methods and the formation process during preparation was investigated. $CeZr_{0.5}Ti_2O_x$ catalyst showed superior redox properties (by H_2-TPR), good adsorption and NO_x/NH_3 activation functions (by NO_x-TPD and NH_3-TPD, respectively), and enhanced charge imbalance (by XPS).

During preparation, the Ti and Zr species were first co-precipitated with an increase in solution pH. Then, the Ce species uniformly precipitated onto the precipitated Zr-Ti species with the further increase in pH. As a result, $CeZr_{0.5}Ti_2O_x$ catalyst with a surface Ce concentration higher than those of Ti and Zr was obtained. This preparation process resulted in the formation of highly-dispersed CeO_2 on ZrO_2-TiO_2, and thus the catalyst can present excellent NH_3-SCR performance.

Author Contributions: W.S. and H.H. conceived the project; Y.G. and Y.Z. performed the experiments; W.S. and Z.L. carried out the data analysis; W.S. and Y.G. wrote the paper; H.H. supervised the study.

Funding: This work was supported by the National Key R&D Program of China (2017YFC0212502, 2017YFC0211101), the National Natural Science Foundation of China (201637005), and the Key Research Program of the Chinese Academy of Sciences (ZDRW-ZS-2017-6-2-3).

Conflicts of Interest: The authors declare no conflicts of interest.

References

1. Parvulescu, V.I.; Granger, P.; Delmon, B. Catalytic removal of NO. *Catal. Today* **1998**, *46*, 233–316. [CrossRef]
2. Granger, P.; Parvulescu, V.I. Catalytic NO_x abatement systems for mobile sources: From three-way to lean burn after-treatment technologies. *Chem. Rev.* **2011**, *111*, 3155–3207. [CrossRef] [PubMed]
3. Liu, Z.; Woo, S.I. Recent advances in catalytic $DeNO_x$ science and technology. *Catal. Rev.* **2006**, *48*, 43–89. [CrossRef]
4. Busca, G.; Lietti, L.; Ramis, G.; Berti, F. Chemical and mechanistic aspects of the selective catalytic reduction of NO_x by ammonia over oxide catalysts: A review. *Appl. Catal. B* **1998**, *18*, 1–36. [CrossRef]
5. Liu, F.; Yu, Y.; He, H. Environmentally-benign catalysts for the selective catalytic reduction of NO_x from diesel engines: Structure-activity relationship and reaction mechanism aspects. *Chem. Commun.* **2014**, *50*, 8445–8463. [CrossRef] [PubMed]
6. Shan, W.; Song, H. Catalysts for the selective catalytic reduction of NO_x with NH_3 at low temperature. *Catal. Sci. Technol.* **2015**, *5*, 4280–4288. [CrossRef]
7. Guan, B.; Zhan, R.; Lin, H.; Huang, Z. Review of state of the art technologies of selective catalytic reduction of NO_x from diesel engine exhaust. *Appl. Therm. Eng.* **2014**, *66*, 395–414. [CrossRef]
8. Gao, F.; Kwak, J.; Szanyi, J.; Peden, C.F. Current understanding of Cu-exchanged chabazite molecular sieves for use as commercial diesel engine $DeNO_x$ catalysts. *Top. Catal.* **2013**, *56*, 1441–1459. [CrossRef]
9. Brandenberger, S.; Kröcher, O.; Tissler, A.; Althoff, R. The state of the art in selective catalytic reduction of NO_x by ammonia using metal-exchanged zeolite catalysts. *Catal. Rev.* **2008**, *50*, 492–531. [CrossRef]
10. Li, J.; Chang, H.; Ma, L.; Hao, J.; Yang, R.T. Low-temperature selective catalytic reduction of NO_x with NH_3 over metal oxide and zeolite catalysts-a review. *Catal. Today* **2011**, *175*, 147–156. [CrossRef]
11. Deka, U.; Lezcano-Gonzalez, I.; Weckhuysen, B.M.; Beale, A.M. Local environment and nature of Cu active sites in zeolite-based catalysts for the selective catalytic reduction of NO_x. *ACS Catal.* **2013**, 413–427. [CrossRef]
12. Li, Y.; Cheng, H.; Li, D.; Qin, Y.; Xie, Y.; Wang, S. WO_3/CeO_2-ZrO_2, a promising catalyst for selective catalytic reduction (SCR) of NO_x with NH_3 in diesel exhaust. *Chem. Commun.* **2008**, 1470–1472. [CrossRef] [PubMed]

13. Can, F.; Berland, S.; Royer, S.; Courtois, X.; Duprez, D. Composition-dependent performance of $Ce_xZr_{1-x}O_2$ mixed-oxide-supported WO_3 catalysts for the NO_x storage reduction–selective catalytic reduction coupled process. *ACS Catal.* **2013**, *3*, 1120–1132. [CrossRef]
14. Long, R.Q.; Yang, R.T. Superior Fe-ZSM-5 catalyst for selective catalytic reduction of nitric oxide by ammonia. *J. Am. Chem. Soc.* **1999**, *121*, 5595–5596. [CrossRef]
15. Chen, L.; Li, J.; Ge, M. Promotional effect of Ce-doped V_2O_5-WO_3/TiO_2 with low vanadium loadings for selective catalytic reduction of NO_x by NH_3. *J. Phys. Chem. C* **2009**, *113*, 21177–21184. [CrossRef]
16. Wu, Z.; Jin, R.; Liu, Y.; Wang, H. Ceria modified MnO_x/TiO_2 as a superior catalyst for NO reduction with NH_3 at low-temperature. *Catal. Commun.* **2008**, *9*, 2217–2220. [CrossRef]
17. Niu, C.; Shi, X.; Liu, K.; You, Y.; Wang, S.; He, H. A novel one-pot synthesized CuCe-SAPO-34 catalyst with high NH_3-SCR activity and H_2O resistance. *Catal. Commun.* **2016**, *81*, 20–23. [CrossRef]
18. Carja, G.; Delahay, G.; Signorile, C.; Coq, B. Fe-Ce-ZSM-5 a new catalyst of outstanding properties in the selective catalytic reduction of NO with NH_3. *Chem. Commun.* **2004**, 1404–1405. [CrossRef] [PubMed]
19. Gao, X.; Jiang, Y.; Fu, Y.; Zhong, Y.; Luo, Z.; Cen, K. Preparation and characterization of CeO_2/TiO_2 catalysts for selective catalytic reduction of NO with NH_3. *Catal. Commun.* **2010**, *11*, 465–469. [CrossRef]
20. Liu, Z.; Yi, Y.; Li, J.; Woo, S.I.; Wang, B.; Cao, X.; Li, Z. A superior catalyst with dual redox cycles for the selective reduction of NO_x by ammonia. *Chem. Commun.* **2013**, *49*, 7726–7728. [CrossRef] [PubMed]
21. Liu, Z.; Zhang, S.; Li, J.; Ma, L. Promoting effect of MoO_3 on the NO_x reduction by NH_3 over CeO_2/TiO_2 catalyst studied with in situ DRIFTS. *Appl. Catal. B* **2014**, *144*, 90–95. [CrossRef]
22. Peng, Y.; Qu, R.; Zhang, X.; Li, J. The relationship between structure and activity of MoO_3-CeO_2 catalysts for NO removal: Influences of acidity and reducibility. *Chem. Commun.* **2013**, *49*, 6215–6217. [CrossRef] [PubMed]
23. Qu, R.; Gao, X.; Cen, K.; Li, J. Relationship between structure and performance of a novel cerium-niobium binary oxide catalyst for selective catalytic reduction of NO with NH_3. *Appl. Catal. B* **2013**, *142*, 290–297. [CrossRef]
24. Shan, W.; Liu, F.; He, H.; Shi, X.; Zhang, C. Novel cerium-tungsten mixed oxide catalyst for the selective catalytic reduction of NO_x with NH_3. *Chem. Commun.* **2011**, *47*, 8046–8048. [CrossRef] [PubMed]
25. Krishna, K.; Seijger, G.B.F.; Bleek, C.M.; Calis, H.P.A. Very active CeO_2-zeolite catalysts for NO_x reduction with NH_3. *Chem. Commun.* **2002**, *18*, 2030–2031. [CrossRef]
26. Shan, W.; Liu, F.; Yu, Y.; He, H. The use of ceria for the selective catalytic reduction of NO_x with NH_3. *Chin. J. Catal.* **2014**, *35*, 1251–1259. [CrossRef]
27. Gu, T.; Liu, Y.; Weng, X.; Wang, H.; Wu, Z. The enhanced performance of ceria with surface sulfation for selective catalytic reduction of NO by NH_3. *Catal. Commun.* **2010**, *12*, 310–313. [CrossRef]
28. Zhang, L.; Pierce, J.; Leung, V.L.; Wang, D.; Epling, W.S. Characterization of ceria's interaction with NO_x and NH_3. *J. Phys. Chem. C* **2013**, *117*, 8282–8289. [CrossRef]
29. Si, Z.; Weng, D.; Wu, X.; Yang, J.; Wang, B. Modifications of CeO_2–ZrO_2 solid solutions by nickel and sulfate as catalysts for NO reduction with ammonia in excess O_2. *Catal. Commun.* **2010**, *11*, 1045–1048. [CrossRef]
30. Si, Z.; Weng, D.; Wu, X.; Ran, R.; Ma, Z. NH_3-SCR activity, hydrothermal stability, sulfur resistance and regeneration of $Ce_{0.75}Zr_{0.25}O_2$–PO_4^{3-} catalyst. *Catal. Commun.* **2012**, *17*, 146–149. [CrossRef]
31. Shen, B.; Wang, Y.; Wang, F.; Liu, T. The effect of Ce-Zr on NH_3-SCR activity over $MnOx(0.6)/Ce_{0.5}Zr_{0.5}O_2$ at low temperature. *Chem. Eng. J.* **2014**, *236*, 171–180. [CrossRef]
32. Ko, J.H.; Park, S.H.; Jeon, J.-K.; Kim, S.-S.; Kim, S.C.; Kim, J.M.; Chang, D.; Park, Y.-K. Low temperature selective catalytic reduction of NO with NH_3 over Mn supported on $Ce_{0.65}Zr_{0.35}O_2$ prepared by supercritical method: Effect of Mn precursors on NO reduction. *Catal. Today* **2012**, *185*, 290–295. [CrossRef]
33. Liu, Z.; Su, H.; Li, J.; Li, Y. Novel MoO_3/CeO_2–ZrO_2 catalyst for the selective catalytic reduction of NO_x by NH_3. *Catal. Commun.* **2015**, *65*, 51–54. [CrossRef]
34. Ding, S.P.; Liu, F.D.; Shi, X.Y.; Liu, K.; Lian, Z.H.; Xie, L.J.; He, H. Significant promotion effect of Mo additive on a novel Ce-Zr mixed oxide catalyst for the selective catalytic reduction of NO_x with NH_3. *ACS Appl. Mater. Interfaces* **2015**, *7*, 9497–9506. [CrossRef] [PubMed]
35. Shan, W.; Liu, F.; He, H.; Shi, X.; Zhang, C. A superior Ce-W-Ti mixed oxide catalyst for the selective catalytic reduction of NO_x with NH_3. *Appl. Catal. B* **2012**, *115–116*, 100–106. [CrossRef]
36. Chen, A.; Zhou, Y.; Ta, N.; Li, Y.; Shen, W. Redox properties and catalytic performance of ceria-zirconia nanorods. *Catal. Sci. Technol.* **2015**, *5*, 4184–4192. [CrossRef]

37. Liu, Z.; Zhang, S.; Li, J.; Zhu, J.; Ma, L. Novel V_2O_5-CeO_2/TiO_2 catalyst with low vanadium loading for the selective catalytic reduction of NO_x by NH_3. *Appl. Catal. B* **2014**, *158–159*, 11–19. [CrossRef]
38. Vuong, T.H.; Radnik, J.; Rabeah, J.; Bentrup, U.; Schneider, M.; Atia, H.; Armbruster, U.; Grünert, W.; Brückner, A. Efficient VO_x/$Ce_{1-x}Ti_xO_2$ catalysts for low-temperature NH_3-SCR: Reaction mechanism and active sites assessed by in situ/operando spectroscopy. *ACS Catal.* **2017**, *7*, 1693–1705. [CrossRef]
39. Wang, Z.; Qu, Z.; Quan, X.; Wang, H. Selective catalytic oxidation of ammonia to nitrogen over ceria–zirconia mixed oxides. *Appl. Catal. A* **2012**, *411–412*, 131–138. [CrossRef]
40. Topsøe, N.-Y. Mechanism of the selective catalytic reduction of nitric oxide by ammonia elucidated by in situ on-line Fourier Transform Infrared Spectroscopy. *Science* **1994**, *265*, 1217–1219. [CrossRef] [PubMed]
41. Lietti, L.; Forzatti, P.; Berti, F. Role of the redox properties in the SCR of NO by NH_3 over V_2O_5-WO_3/TiO_2 catalyst. *Catal. Lett.* **1996**, *41*, 35–39. [CrossRef]
42. Geng, Y.; Huang, H.; Chen, X.; Ding, H.; Yang, S.; Liu, F.; Shan, W. The effect of Ce on a high-efficiency CeO_2/WO_3-TiO_2 catalyst for the selective catalytic reduction of NO_x with NH_3. *RSC Adv.* **2016**, *6*, 64803–64810. [CrossRef]
43. Liu, F.; He, H. Structure-activity relationship of iron titanate catalysts in the selective catalytic reduction of NO_x with NH_3. *J. Phys. Chem. C* **2010**, *114*, 16929–16936. [CrossRef]
44. Bêche, E.; Charvin, P.; Perarnau, D.; Abanades, S.; Flamant, G. Ce 3d XPS investigation of cerium oxides and mixed cerium oxide ($Ce_xTi_yO_z$). *Surf. Interface Anal.* **2008**, *40*, 264–267. [CrossRef]
45. Liu, C.; Chen, L.; Chang, H.; Ma, L.; Peng, Y.; Arandiyan, H.; Li, J. Characterization of CeO_2-WO_3 catalysts prepared by different methods for selective catalytic reduction of NO_x with NH_3. *Catal. Commun.* **2013**, *40*, 145–148. [CrossRef]
46. Shan, W.; Liu, F.; He, H.; Shi, X.; Zhang, C. An environmentally-benign CeO_2-TiO_2 catalyst for the selective catalytic reduction of NO_x with NH_3 in simulated diesel exhaust. *Catal. Today* **2012**, *184*, 160–165. [CrossRef]